New prediction for wave length selection of radial fingering in a Hele-Shaw cell

M. Nagel, F. Gallaire

Laboratoire de Mécanique des Fluides et Instabilités, EPFL STI-IGM, Station 9, CH-1015 Lausanne, Suisse

Résumé :

Les analyses de stabilité existantes sur la digitation visqueuse en cellule de Hele-Shaw par injection radiale d'un fluide peu visqueux dans un fluide plus visqueux reposent sur le modéle de Darcy. La comparaison entre les résultats qui en découlent et les expériences révèlent de grandes différences lorsque le nombre capillaire s'approche de 1. Dans cette étude, nous utilisons les équations de Brinkman pour décrire l'écoulement. Nous montrons que les contraintes planaires jouent un rôle dominant dans la détermination du mode le plus instable lorsque la tension de surface devient petite en comparaison aux effets visqueux.

Abstract :

Existing linear stability analysis of radial fingering in Hele-Shaw cells use Darcy's law as a model for the fluid motion. Comparison between experiments and theory reveals a large discrepancy at order 1 capillary numbers. In this work we use the so-called Brinkman equations to describe the fluid motion. It becomes apparent that the in-plane stresses play a dominant role in the determination of the most unstable mode as the surface tension gets very small.

Mots clefs : **Saffman-Taylor instability, Hele-Shaw cell, radial fingering**

1 Introduction

The fingering instability was first discussed in 1958 by Taylor and Saffman [1]. They considered two fluids separated by a flat interface in a shallow channel, called Hele-Shaw cell. When the less viscous fluid displaces the more viscous fluid the formation of fingers is observed. In 1981, Paterson [2] analyzed by linear stability analysis radial fingering in a Hele-Shaw cell, when a less viscous fluid is injected in the center of a more viscous fluid. He determined the most unstable modes by estimating the maximum growth rates for different Capillary numbers. The Capillary number is a dimensionless number that compares viscous forces against surface forces,

$$Ca = \frac{\mu U}{\gamma}.$$

In a series of experiments, Maxworthy [3] showed in 1989 that for high Capillary number the number of expected fingers is larger than found in his observations. Already in 1984 Park and Homsy [4] derived corrected boundary conditions for viscous displacement based on a double asymptotic expansion for a small gap width and small Capillary number. Later the same year Park, Homsy and Gorell performed an experiment for the displacement of a flat interface [5] and compared these results with a linear stability analysis, which showed good agreement for low Capillary numbers. Their derived boundary conditions take into account the inhomogeneous in-plane curvature over the height of the channel. Laplace law for the depth averaged profile becomes

$$[\![p]\!] = \gamma\Big(\frac{\pi}{4}\kappa + \frac{2}{h}\Big),$$

with channel height h and apparent in-plane curvature κ.

At very low Capillary number this development matches even better to Maxworthy's experiments than Paterson's prediction but the discrepancy for higher Capillary number increased. Recently Kim et al. [6] used a formulation based on Darcy's law but included viscous normal stresses at the interface. This procedure did closely match the results of Maxworthy also for Capillary number around 1, but the justification to assume normal stresses only at the interface seems however somewhat arbitrary.

If the Capillary number becomes order 1 or larger, hence when the surface tension vanishes, for example in miscible flows with low diffusivity, the theory shows for increasing wave number increasing growth rates without bound. Paterson had discussed this issue already in 1985 [7] where he derived a cut-off wavelength based on the argument that the flow conditions at the interface are three-dimensional and he analysed for which wave length the dissipation is minimized. He found the cut-off wave length to be only dependent on the aspect ratio, height to radius.

A different approach is presented in a very recent work by Logvinov et al. [8], following a very similar approach to the one described herein. They considered the displacement of a flat interface without surface tension and recover a wave length selection due to viscous in-plane stresses.

Note that a similar approach has been followed by [9, 10, 11] to study the Kelvin-Helmholtz instability in Hele-Shaw cells, where they employ Euler equations with a friction term in the shallow direction leading to the so the called Euler-Darcy equations.

2 Linear stability analysis

Darcy's law transforms the problem into 2D potential flow. Starting from Navier-Stokes first the inertial terms are discarded, leading to the Stokes equation. Because of the small channel height, viscous stresses in the plane are neglected and only kept in the shallow direction. The velocity profile in the small direction is assumed to be a Poiseuille profile, a parabola, and can therefore be integrated and depth-averaged. The viscous constraint is then only dependent on the averaged in-plane velocities and not on their derivatives. Taking the divergence of the momentum equations transforms the pressure into a potential Φ, scaled by viscosity μ and parameter k from depth averaging :

$$\Delta p = \mu\, k^2\, \Delta\Phi = 0, \quad \nabla\Phi = \vec{u}, \quad k = \sqrt{12}\, R/h.$$

The aspect ratio k uses the height of the channel h, normalized the radius of the droplet R. When transformed into polar coordinates Paterson uses exponentials as general solutions to solve analytically for the growth rates.

In contrast to Darcy's law, Brinkman equations do not neglect the in-plane stresses. After depth-averaging the Stokes equations one obtains :

$$\mu\Big(\Delta\vec{u} - \frac{k^2}{R^2}\vec{u}\Big) - \nabla p = 0, \tag{1}$$

$$\mathrm{div}(\vec{u}) = 0. \tag{2}$$

This equation does not have a potential because the vorticity is non zero. The equation can be transformed into polar coordinates using u and v as radial and angular velocity components. From here on we will only use dimensionless variables.

The dimensionless momentum equations in r and θ direction :

$$\Big(\frac{\partial^2 u}{\partial r^2} + \frac{\partial u}{r\partial r} + \frac{\partial^2 u}{r^2\partial\theta^2} - \frac{u}{r^2} - k^2 u - \frac{2\partial v}{r^2\partial\theta}\Big) - \frac{\partial p}{\partial r} = 0 \tag{3}$$

$$\Big(\frac{\partial^2 v}{\partial r^2} + \frac{\partial v}{r\partial r} + \frac{\partial^2 v}{r^2\partial\theta^2} - \frac{v}{r^2} - k^2 v + \frac{2\partial u}{r^2\partial\theta}\Big) - \frac{\partial p}{r\partial\theta} = 0. \tag{4}$$

Taking the curl of equation 1, replacing u and v by the stream function and transformation into polar coordinates one arrives at :

$$u = -\frac{\partial \Psi}{r\partial\theta}, \quad v = \frac{\partial \Psi}{\partial r},$$
$$\Big(\frac{\partial}{r\partial r} r \frac{\partial}{\partial r} + \frac{\partial^2}{r^2 \partial\theta^2}\Big)\Big(\frac{\partial}{r\partial r} r \frac{\partial}{\partial r} + \frac{\partial^2}{r^2 \partial\theta^2} - k^2\Big)\Psi = 0. \tag{5}$$

The base flow for a radially evolving liquid is constructed using the incompressibility equation. Since the base flow depends only on the radial direction the pressure can be integrated using eq. (3), which gives :

$$u_0 = \frac{1}{r}, \quad v_0 = 0 \quad \text{and} \quad p_{0j} = -\tilde{\mu}_j k^2 \ln(r) + P_{0j}.$$

Where we used dimensionless viscosities $\tilde{\mu_i}$ defined as :

$$\tilde{\mu}_i = \frac{\mu_i}{\mu_1 + \mu_2}.$$

The solution for the pressure field is valid in the inner and outer fluid up to a constant, which matches the pressure jump due to surface tension at the interface. The bottom indices identify on the first digit the order of expansion, for which zero corresponds to the base flow, and second digit corresponding to 1 - inside and 2 - outside.

For the perturbation the general solution for eq. (5) is used. There exist infinitely many solutions corresponding to different wave numbers of perturbations at the interface. The fourth order equation has 4 unknowns for every wavenumber, of which two can be excluded as to fulfill the boundary conditions either at the origin or at infinity.
The inner solution is of form :

$$\Psi_{11} = \Big(a\frac{I_n(kr)}{I_n(k)} + b\, r^n\Big)e^{in\theta}, \tag{6}$$

and the outer :

$$\Psi_{12} = \Big(c\frac{K_n(kr)}{K_n(k)} + d\, r^{-n}\Big)e^{in\theta}. \tag{7}$$

The parameters a,b,c and d have to be determined from the boundary conditions at the interface. The structure of eq. (5) shows as mentioned that the classical solutions of the Laplace equation are also solutions of the Brinkman equation. The second bracket in eq. (5) adds two distinct solutions, which contain the modified Bessel functions K_n and I_n. The interface position itself being a wave like perturbation, with a time dependent amplitude f :

$$\alpha = i\, e\, f(t) e^{in\theta}, \tag{8}$$

where e is the perturbation of the interface.

Five conditions are to be imposed at the interface : Equality of radial, tangential and interface velocity, continuity of tangential stress and jump of normal stress due to curvature and surface tension. The flattened boundary conditions at the interface consider the first order Taylor expansions around the original interface position. All perturbation quantities will be inserted with a ϵ to denote that they are much smaller than the base flow. For the inner radial velocity moving with the interface :

$$\frac{\partial(R(t) + \epsilon\alpha(t))}{\partial t} = u_{0j} + \epsilon u_{1j} + \epsilon \frac{\partial u_{0j}}{\partial r}\alpha \tag{9}$$

The first term on the left hand side and the first term on the right hand side cancel out because the base flow drives the interfacial displacement. Substituting the perturbation stream function for the perturbation velocity :

$$\frac{\partial \alpha(t)}{\partial t} = -\frac{\partial \Psi_{1j}}{r\partial\theta} + \frac{\partial u_{0j}}{\partial r}\alpha \tag{10}$$

Matching the outer velocity to the inner velocity at the interface :

$$\frac{\partial \Psi_{11}}{\partial \theta} = \frac{\partial \Psi_{12}}{\partial \theta}. \tag{11}$$

The equality of tangential velocities on the flattened interface is expressed as :

$$\frac{\partial \Psi_{11}}{\partial r} = \frac{\partial \Psi_{12}}{\partial r}. \tag{12}$$

The normal and tangential stress components at the interface are taken from the Brinkman equations. Since the surface stress component in the shallow direction is averaged out, only the radial stress σ_{rr} and the in-plane tangential stress $\sigma_{r\theta}$ are matched.

To ensure continuity of the tangential stress at the interface :

$$\tilde{\mu}_1\Big(-\frac{\partial^2}{r^2\partial\theta^2}\Psi_{11} + r\frac{\partial}{\partial r}\Big(\frac{\partial}{r\partial r}\Psi_{11}\Big)\Big) - \tilde{\mu}_2\Big(-\frac{\partial^2}{r^2\partial\theta^2}\Psi_{12} + r\frac{\partial}{\partial r}\Big(\frac{\partial}{r\partial r}\Psi_{12}\Big)\Big) = 0. \tag{13}$$

Continuity of the normal stress balance is more involved since it requires to recover the pressure, which had been left out in the calculation. Integrating eq. (4) for θ relates the pressure perturbations to the general solutions.

$$p_{1j} = \tilde{\mu}_j r \int_0^\theta \Big(\frac{\partial^3 \Psi_{1j}}{\partial r^3} + \frac{\partial^2 \Psi_{1j}}{r\partial r^2} - \Big(\frac{n^2}{r^2} + k^2 + \frac{1}{r^2}\Big)\frac{\partial \Psi_{1j}}{\partial r} + \frac{2n^2}{r^3}\Psi_{1j}\Big)d\theta \tag{14}$$

The relations read :

$$p_{11} = -b\,\tilde{\mu}_1 r^n\, k^2 e^{in\theta}, \quad \text{and} \quad p_{12} = d\,\tilde{\mu}_2 r^{-n} k^2 e^{in\theta}.$$

The radial stress balance in order ϵ for the flattened interface reads :

$$p_{11} + \frac{\partial p_{01}}{\partial r}\alpha + 2\tilde{\mu}_1\frac{\partial}{\partial r}\Big(\frac{\partial}{r\partial\theta}\Psi_{11}\Big) - 2\tilde{\mu}_1\frac{\partial^2 u_0}{\partial r^2}\alpha$$

$$-p_{12} - \frac{\partial p_{02}}{\partial r}\alpha - 2\tilde{\mu}_2\frac{\partial}{\partial r}\Big(\frac{\partial}{r\partial\theta}\Psi_{12}\Big) + 2\tilde{\mu}_2\frac{\partial^2 u_0}{\partial r^2}\alpha = -\frac{\pi}{4\,Ca}\Big(\alpha + \frac{\partial^2\alpha}{\partial\theta^2}\Big). \tag{15}$$

3 Dispersion relation

The dispersion relation is found by requiring that the obtained linear system of five equations has a non trivial solution. Under the prerequisite that the inner viscosity is zero, the modified Bessel functions of first kind I cancels out and an expression involving only K_n and K_{n+1} is left. The dispersion relation can be rearranged as follows :

$$\frac{df}{f\,dt} = \frac{A(k,n) + \frac{\pi}{4}\mathrm{Ca}^{-1}\,B(k,n)}{C(k,n)}. \tag{16}$$

In this form it can be easily seen that the growth rate depends on a certain parameter pairing, where $A(k,n)$ represents the flow rate and $B(k,n)$ represents the influence of surface tension. The parametric functions are :

$$A(k,n) = k^4n - k^4 - 8n^2 - 8n^4 + 4k^2n - 8k^2n^2 + \frac{K_{n+1}(k)}{K_n(k)}(-2k^3 + 2k^3n + 4kn + 4kn^3), \tag{17}$$

$$B(k,n) = k^2n - k^2n^3 + 4n^4 - 4n^2 + \frac{K_{n+1}(k)}{K_n(k)}(2kn - 2kn^3), \tag{18}$$

$$C(k,n) = k^4 - 8n^2 + 8n^4 + 4k^2n^2 + \frac{K_{n+1}(k)}{K_n(k)}(2k^3 - 4kn^3 + 4kn). \tag{19}$$

A closer look at the parametric functions will already give insights into the mechanisms at work. For a better comparison with existing results we will decompose the growth rate ω obtained by Paterson [2] in the same way. We will only correct the influence of surface tension by factor $\pi/4$, which is the corrected boundary condition according Park and Homsy. Taking

$$\frac{df}{f\,dt} = (n-1) - \frac{\pi}{4}\frac{n(n^2-1)}{\mathrm{Ca}\,k^2}, \tag{20}$$

and reorganizing it for eq. (16) one obtains :

$$A'(k,n) = (n-1)k^4, \quad B'(k,n) = n(1-n^2)k^2 \quad \text{and} \quad C'(k,n) = k^4.$$

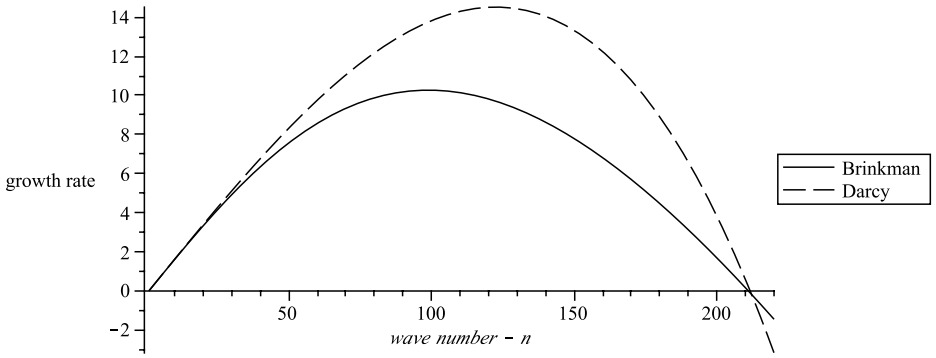

FIGURE 1 – Example of a dispersion relation for k = 300 and Ca = 0.5

To leading order in aspect ratio k the parameters found using the Brinkman model recovers the results of Paterson. However it is apparent that, where Paterson's pairing of $A'(k,n)/C'(k,n)$ grows linearly with n, our relation has stabilizing terms that grow faster in wave number n than the destabilizing terms. This ensures that for finite aspect ratio k, there will always be a finite cut-off wave number n.

Plotting the differential growth $\frac{df}{f\,dt}$ against the wave number for the set of parameters of figure 1 shows two properties in the dispersion relation induced by the Brinkman model :

– The growth rates are smaller for all wave lengths.
– The maximum growth rates shift to lower wave numbers as higher modes receive larger damping.

In figure 2 the most unstable wave numbers as plotted by Maxworthy are shown, including the results from our stability analysis. Maxworthy chose to plot the results for a modified wave number being

$$A_{max} = \sqrt{\frac{12}{\mathrm{Ca}}}\,\frac{n_{max}}{k},$$

because Paterson's result are represented as a straight line. With the corrected boundary conditions of Park and Homsy this line should be constantly 2.26 for all Capillary numbers. Maxworthy showed, as the Capillary number approaches unity the observed number of fingers becomes much smaller than predicted by Paterson. Our findings are dash-dot line and show an improved matching.

Although we invoke an additional scale by considering the in-plane stresses, the dominant modified wave number remains solely dependent on the Capillary number and does not vary for different aspect ratios k.

4 Conclusions

The new dispersion relation covers a wide range of Capillary numbers and shows a good approximation with experiments. The decreased wave number of the maximal growth is achieved by keeping the in-plane stresses. When the surface tension has only little influence the in-plane stresses stabilize for high wave numbers. The high wave number create large velocity gradients and thus shear stresses at the interface. Darcy's law can not account for them, in contrast to the Brinkman model, which allows for a cut-off wave number even with zero surface tension.

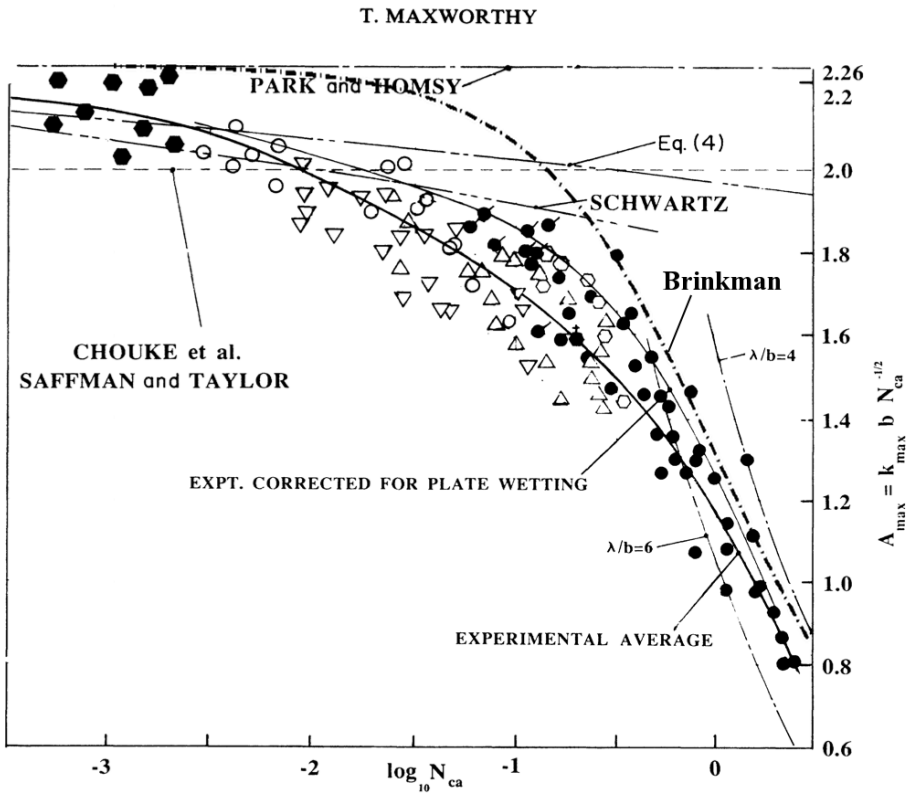

FIGURE 2 – Wave number selection as compiled by Maxworthy together with our findings as dash-dot line.

Références

[1] Saffman, P. G., Taylor, G. I. 1958 The Penetration of a Fluid into a Porous Medium or Hele-Shaw Cell Containing a More Viscous Liquid. *Proc. Roy. Soc. A* **245** (1242) 312-329

[2] Paterson, L. 1981 Radial fingering in a Hele Shaw cell. *J. Fluid Mech.* **113** 513-529

[3] Maxworthy, T. 1989 Experimental study of interface instability in a Hele-Shaw cell. *Phys. Rev. A*, **39** (11) 5863-5866

[4] Park, C.-W., Homsy, G. M. 1984 Two-phase displacement in Hele Shaw cells : theory. *J. Fluid Mech.* **139** 291-308

[5] Park, C.-W., Gorell, S., Homsy G. M. 1984 Two-phase displacement in Hele-Shaw cells : experiments on viscously driven instabilities. *J. Fluid Mech.* **141** 275-287

[6] Kim, H., Funada, T., Joseph, D. D., Homsy, G. M. Viscous potential flow analysis of radial fingering in a Hele-Shaw cell. *Phys. Fluids* **21** 074106

[7] Paterson, L. 1985 Fingering with miscible fluids in a Hele Shaw cell. *Phys. Fluids*, **28** (1) 26-30

[8] Logvinov, O. A., Ivashnyov, O. E., Smirnov, N. N. 2010 Evaluation of viscous fingering width in Hele-Shaw flows. *Acta Astronautica* **67** 53-59

[9] Gondret, P., Rabaud, M. 1997 Shear instability of two-fluid parallel flow in a Hele-Shaw cell. *Phys. Fluids* **9** (11) 3267-3274

[10] Gondret, P., Ern, P., Meignin, L., Rabaud, M. 1999 Experimental Evidence of a Nonlinear Transition from Convective to Absolute Instability. *Phys. Rev. Letter.* **82** 1442-1446

[11] Plouraboué, F., Hinch, E. J. 2002 Kelvin-Helmholtz instability in a Hele-Shaw cell. *Phys. Fluids* **14** (3) 922-929